Int. J. Electrochem. Sci., 13 **(2018)** 11273 – 11285, doi: 10.20964/2018.11.90

International Journal of
ELECTROCHEMICAL
SCIENCE
www.electrochemsci.org

Corrosion Inhibition of Carbon Steel by Lepidine in HCl Solution

*Wenheng Huang, Lingyu Hu, Chunmiao Liu, Jie Pan, Yang Tian, Kun Cao**

Department of Chemistry & Chemical Engineering, Neijiang Normal University, Neijiang, Sichuan, 641112, PR China
*E-mail: kevin_cao0811@126.com

Received: 24 July 2018 / *Accepted:* 3 September 2018 / *Published:* 1 October 2018

Carbon steel is an important metal for structure and machines, and it is easily corroded in acidic media. In this paper, lepidine was used as a corrosion inhibitor for carbon steel in 1 mol/L HCl solution. A weight loss test and electrochemical methods were used to study the inhibition performance at different temperatures; surface analysis and a thermodynamic method were used to clarify the corrosion inhibition mechanism. In the weight loss test, when the corrosion inhibitor was added, the corrosion rate was decreased from 12.54 mg cm^{-2} h^{-1} to 0.113 mg cm^{-2} h^{-1}, and the rate of corrosion inhibition was 99.1%. Furthermore, the corrosion inhibition efficiency decreased with an increase in temperature. From the polarization curve test, the corrosion potential of the corrosion inhibitor was moving forward to cathode as concentration increased, and the cathode current density decreased obviously. From EIS, the radius of the resistance of the corrosion inhibitor was found to increase gradually with an increase in concentration. With an increase in concentration, R_{ct} increased and C_{dl} decreased, showing that the corrosion inhibitors replaced water and adsorbed onto the film. Adsorption of the corrosion inhibitor obeyed the Langmuir isothermal adsorption equation, and SEM and XPS proved this hypothesis. Adsorption of the inhibitor on the surface of carbon steel is a spontaneous exothermic process.

Keywords: Corrosion inhibitor; Electrochemical methods; Carbon steel; Lepidine; Langmuir isothermal adsorption

1. INTRODUCTION

Carbon steel plays an important role in infrastructure and industrial facilities because of its excellent thermal conductivity, ductility, and good cost-effectiveness ratio. Fe atoms easily react with oxygen in humid air and form a layer of rust on the surface of metal. The rust is usually removed with a hydrochloric acid solution. To avoid or slow the excessive consumption of metals in pickling processes, a corrosion inhibitor is an important additive in acid solution[1,2]. Commonly used organic corrosion inhibitors contain sulfur, nitrogen, or aromatic and unsaturated bonds in the molecular structure, and these provide active adsorption centers, cause the inhibitor molecules to adsorb on the metal surface, and endow compounds with high corrosion inhibition performance[3-8].

In the literature, quinoline and its derivatives have been investigated as corrosion inhibitors for many commercial metals because of the p-π conjugation of the quinoline ring[9-12]. Singh used four kinds of quinoline derivatives as inhibitors for carbon steel in 1.0 mol/L HCl solution, and the results showed that the corrosion inhibitors had high inhibition efficiency because of the formation of a monolayer on the surface of carbon steel[13]. Lgaz studied three quinoline derivatives using electrochemical methods and molecular dynamic simulations. The results showed that the inhibitors have excellent anticorrosion performance and that their adsorption on a metal surface obeyed the Langmuir adsorption model. Electrochemical results indicated that quinoline derivatives behave as mixed-type inhibitors. These inhibitors increased the polarization resistance and simultaneously lowered the double layer capacitance[14].

In this study, lepidine (4-methylquinoline) was used as a corrosion inhibitor for carbon steel in 1 mol/L HCl solution. Electrochemical techniques and theoretical studies were conducted to assess corrosion inhibition efficiency.

2. EXPERIMENTAL

2.1 Reagent and sample pre-processing

Lepidine was supplied by Adamas Pharmaceuticals Inc. The concentration of Lepidine ranged from 0.1 mmol/L to 10 mmol/L in 1 mol/L HCl solution. The working electrode and weight loss samples were carbon steel that was cut into cubes with a side length of 10 mm and sheet area of 50 mm×25 mm×3 mm. All of the samples were abraded using sandpaper from 200# to 1200#, then successively washed with deionized water and ethanol, and dried with nitrogen.

2.2 Weight loss test

The weight loss test was carried out at 25°C, 35°C, 45°C, 55°C, and 65°C. All specimens were immersed in 1 mol/L HCl solution for 3 h without or with lepidine. After that, all of the specimens were taken out of the solution, rinsed in distilled water and ethanol, and finally dried and weighed after 24 h. The corrosion rate (C_{RW}, mg cm^{-2} h^{-1}), surface coverage rate θ, and inhibition efficiency (η_W) were calculated using the following equations:

$$C_{RW} = \frac{W_1 - W_2}{St} \qquad \text{(eq. 1)}$$

$$\theta = \frac{C_{RW}^0 - C_{RW}}{C_{RW}^0} \qquad \text{(eq. 2)}$$

$$\eta_W\% = \frac{C^0_{RW} - C_{RW}}{C^0_{RW}} \times 100 \qquad \text{(eq. 3)}$$

where W_1 and W_2 are the weights of carbon steel immersed in the solution without and with inhibitor, respectively. S is the surface area of the specimen. t is the immersion time. C^0_{RW} and C_{RW} are the corrosion rates of carbon steel in the solution without and with inhibitor, respectively.

2.3. Electrochemical experiments

An Ivium electrochemical workstation and a three-electrode cell system were used for the electrochemical tests. Carbon steel, a platinum electrode, and a saturated calomel electrode (SCE) with a Luggin capillary were used as the working electrode, counter electrode, and reference electrode, respectively.

EIS plots were obtained at frequencies from 100 kHz to 10 mHz and analyzed using Zsimpwin software. Polarization curves were scanned from -700 to -200 mV (versus SCE), and the scanning rate was 5 mV/s. The inhibition efficiency based on corrosion current density or charge transfer resistance was calculated using eqs. 4 and 5

$$\eta_{\mathrm{i}} = \frac{i^0_{\mathrm{corr}} - i_{\mathrm{corr}}}{i^0_{\mathrm{corr}}} \times 100\% \qquad \text{(eq. 4)}$$

$$\eta_{\mathrm{R}} = \frac{R_{\mathrm{ct}} - R^0_{\mathrm{ct}}}{R_{\mathrm{ct}}} \times 100\% \qquad \text{(eq. 5)}$$

where i_{corr} and i^0_{corr} are the corrosion current densities of carbon steel with and without the inhibitor, respectively, in 1 mol/L HCl solution. R_{ct} and R^0_{ct} represent the resistances of charge transfer with and without the inhibitor, respectively.

2.4. Surface analysis

After pre-processing, carbon steel specimens were immersed in 1 mol/L HCl solution without or with 10 mmol/L lepidine for 24 h, then washed with deionized water, and dried with nitrogen. A TEDCAN VEGA 3 SBH model scanning electron microscope was used to record the surface morphology of the sample, and the chemical composition of the adsorption film was analyzed using X-ray photoelectron spectroscopy (PHI-5400 model) using Al Kα as the radiation source.

3. RESULTS AND DISCUSSION

3.1 Weight loss test

Table 1 shows the corrosion rate and corrosion inhibition efficiency of carbon steel in HCl solution at different temperatures. As seen in Table 1, adding inhibitor remarkably decreased the corrosion rate, and the corrosion inhibition efficiency increased with an increase in the concentration of the inhibitor. The inhibition efficiency reached a maximum value of 99.1% at a concentration of 10 mmol/L at 298K and decreased to 81.8% at 338K, which could be because of the accompanying decrease in adsorption and increase in inhibitor desorption from the metal surface[15-17].

Table 1. Corrosion parameters of carbon steel immersed in 1 M HCl solution in the absence and presence of different concentrations of inhibitor at different temperatures

T (℃)	C （mmol/L）	Lepidine		
		C_{RW} (mg cm^{-2} h^{-1})	θ	η_W （%）
25	0	12.54	-	-
	0.1	6.208	0.50	50.5
	0.5	1.971	0.84	84.3
	1	0.852	0.93	93.2
	5	0.172	0.99	98.6
	10	0.113	0.99	99.1
35	0	14.73	-	-
	0.1	9.325	0.37	36.7
	0.5	4.832	0.67	67.2
	1	2.122	0.86	85.6
	5	1.123	0.92	92.4
	10	0.839	0.94	94.3
45	0	16.81	-	-
	0.1	11.12	0.34	33.8
	0.5	8.888	0.47	47.1
	1	4.942	0.71	70.6
	5	1.835	0.89	89.1
	10	1.229	0.93	92.7
55	0	21.73	-	-
	0.1	17.53	0.19	19.3
	0.5	13.79	0.37	36.5
	1	10.28	0.53	52.7
	5	6.214	0.71	71.4
	10	2.567	0.88	88.2
65	0	29.36	-	-
	0.1	23.82	0.19	18.9
	0.5	19.81	0.33	32.5
	1	13.56	0.54	53.8
	5	9.467	0.68	67.7
	10	5.329	0.82	81.8

3.2 EIS measurement

Electrochemical impedance spectroscopy diagrams of carbon steel without and with the addition of lepidine are presented as Nyquist plots (Fig. 1). As seen in Fig. 1, all of the impedance spectra exhibit a single irregular depressed capacitive loop, and this suggests that corrosion of carbon steel in 1 M HCl is controlled by a charge transfer process at the interface between the electrode surface and liquid in all of the cases examined here[18]. With the addition of lepidine in the solution, the shape of the impedance spectra did not change; with an increase in the concentration of the inhibitor, the radius increased, which indicates that the inhibitor controlled the activity of the corrosion reaction rather than altering the corrosion mechanism[19]. In addition, the irregular depressed capacitive loop corresponded to the frequency dispersion of the interfacial impedance, which is correlated to the surface inhomogeneity of solid electrodes and the chemical heterogeneity of the surface[20]. An equivalent electrical circuit is shown in Fig. 2 and was used to fit the impedance. This equivalent circuit model can be used to determine the solution resistance (R_s), charge transfer resistance (R_{ct}), and electrical double layer capacitance (C_{dl}). The double layer at the interface was not an ideal capacitor, and thus, a constant phase element was introduced to replace the double layer. The impedance of the CPE and the double layer capacitances C_{dl} were expressed as eqs. 6 and 7[21], where Y_0 is a proportionality coefficient, $j^2= -1$ is an imaginary number, ω is the angular frequency, and n is the phase shift. The phase shift corresponds to the degree of surface inhomogeneity[22,23].

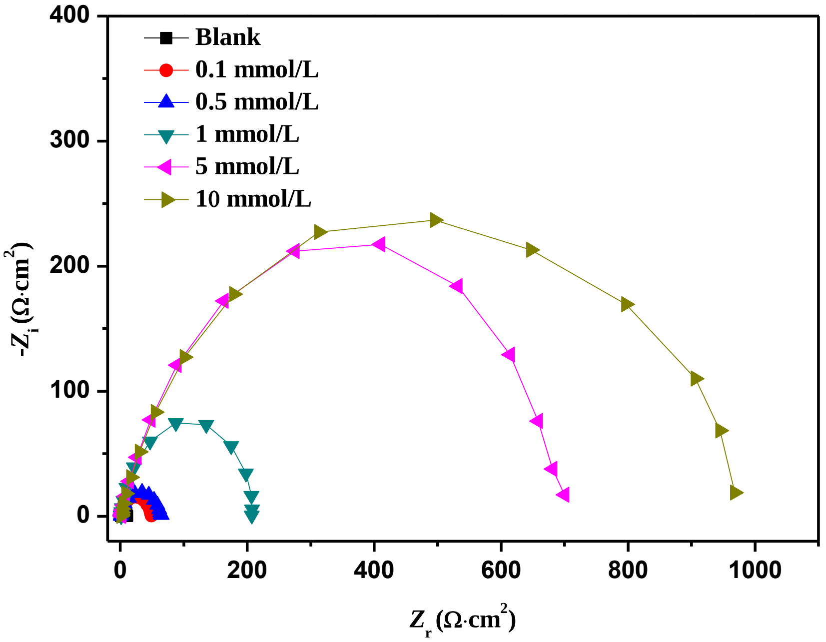

Figure 1. Nyquist plots of carbon steel in 1 mol/L HCl solution with different concentrations of inhibitor.

According to the value of n, when n=0 and Y0=R, CPE behaves as a resistance. When n=1 and Y0=C, CPE represents capacitance. When n=-1 and Y0=L, CPE is inductance. When n=0.5 and Y0=W, CPE is Warburg impedance.

$$Q_{CPE} = Y_0^{-1}\left(j\omega\right)^{-n} \quad \text{(eq. 6)}$$

$$C_{dl} = Y_0\left(\omega_m\right)^{n-1} \quad \text{(eq. 7)}$$

Inhibition efficiency and other fitted impedance parameters are shown in Table 2. Analysis of the impedance results in Table 2 shows that R_{ct} increased and C_{dl} decreased with the addition of inhibitors in 1 mol/L HCl solutions, and the trends are more obvious with an increase in the concentration of inhibitors. An increase in R_{ct} demonstrates the improved protection effects of the inhibitor, and a slowly corroding system. The slowly corroding system results from the gradual replacement of water molecules by quinoline molecules on the surface, and this consequently leads to a decrease in the number of active sites necessary for the corrosion reaction[24,25]. The decreased C_{dl} values indicate that the charge and discharge rates to the metal-solution interface were greatly decreased.

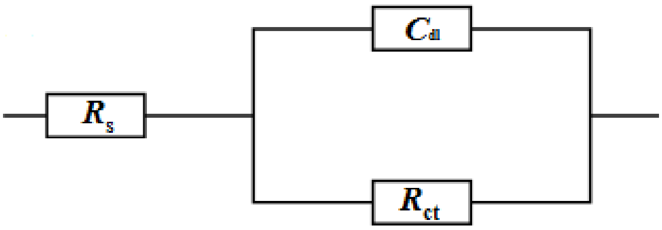

Figure 2. Equivalent circuit of the Nyquist plots.

Table 2. Impedance parameters of carbon steel in 1 mol/L HCl solution with different concentrations of inhibitor at 298K

C (mmol/L)	R_s (Ω cm^2)	C_{dl} (μF/cm^2)	n	R_{ct} (Ω cm^2)	η_R (%)
0	0.9591	266	0.86	9.681	—
0.1	1.17	225	0.88	28.66	66.2
0.5	0.7616	170	0.88	86.05	88.8
1	1.104	145	0.89	183.3	94.7
5	0.9751	86	0.87	829	98.8
10	1.377	40	0.88	1154	99.2

3.3 Potentiodynamic polarization curves

Potentiodynamic polarization curves are shown in Fig. 3 for mild steel in 1 M HCl without and with various concentrations of inhibitor. Electrochemical parameters such as corrosion potential (E_{corr}), corrosion current density (i_{corr}), corrosion inhibition efficiency (η_i), anodic Tafel slope (β_a), and cathodic Tafel slope (β_c) are presented in Table 3. As seen in the potentiodynamic polarization curves, I_{corr} and E_{corr} decrease with an increase in inhibitor concentration. The corrosion potential (E_{corr}) values did not shift more than 85 mV with respect to the corrosion potential of the blank solution, and this suggests that the inhibitor acted as a mixed type[26,27]. As seen in Fig. 3, the addition of inhibitor reduces both the cathodic and anodic currents and therefore hinders the acid attack of the mild steel electrode in 1 mol/L HCl; also, the cathodic Tafel slopes (β_c) and anodic Tafel slopes (β_a) were obtained by extrapolation, and the value barely changed with the inhibitor concentration, which reveals that the inhibitor has a significant effect and is effective at inhibiting the hydrogen evolution reaction on the cathode and slows the dissolution rate of carbon steel. This proved that the inhibitor adsorbed onto the steel surface and constructed a film that hindered the active sites[28,29].

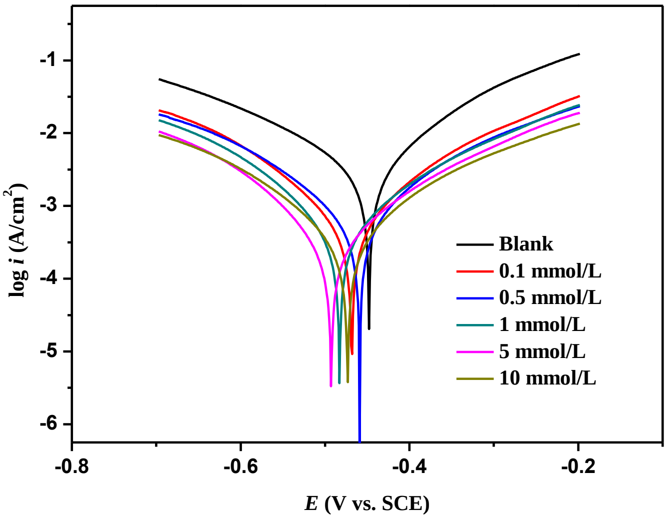

Figure 3. Potentiodynamic polarization curves of carbon steel in 1 mol/L HCl solution with different concentrations of inhibitor.

Table 3. Potentiodynamic polarization parameters of carbon steel in 1 mol/L HCl solution with different concentrations of inhibitor

C (mmol/L)	*E* (V vs. SCE)	*i* (mA/cm^2)	β_c (mV/dec)	β_a (mV/dec)	η_i （%）
0	-448	1.156	-20.2	22.1	—
0.1	-467	0.285	-21.3	22.0	75.3
0.5	-458	0.209	-20.9	21.3	81.9
1	-492	0.192	-22.1	18.7	83.4
5	-499	0.163	-18.9	21.5	85.9
10	-481	0.149	-19.7	21.2	87.1

3.4 Adsorption isotherm

Adsorption of lepidine on the surface of carbon steel is important and can be further understood from adsorption isotherms[30]. According to four adsorption isotherms, the Langmuir adsorption isotherm was the best fitted adsorption model. The relationship of θ and C obeyed the following equations：

$$\frac{C}{\theta} = \frac{1}{K_{ads}} + C \qquad \text{(eq. 8)}$$

$$\Delta G^0_{\text{ads}} = -RT\ln\left(55.5K_{\text{ads}}\right) \qquad \text{(eq. 9)}$$

K_{ads} is the equilibrium constant of the adsorption-desorption process, ΔG^0_{ads} is the standard free energy of adsorption.

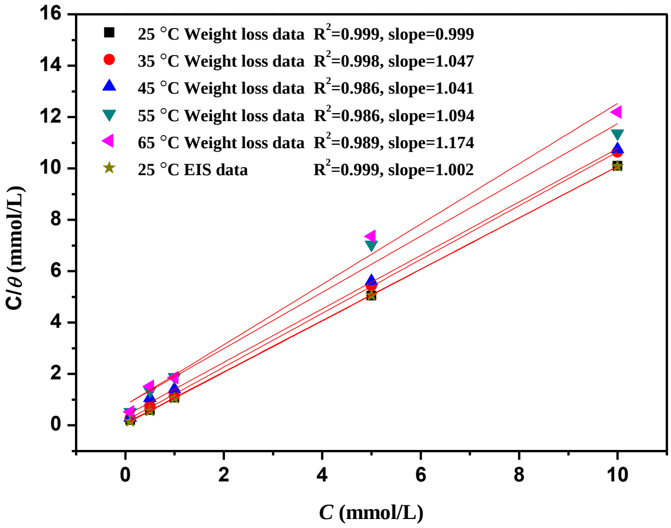

Figure 4. Langmuir adsorption isotherms of carbon steel in HCl solution.

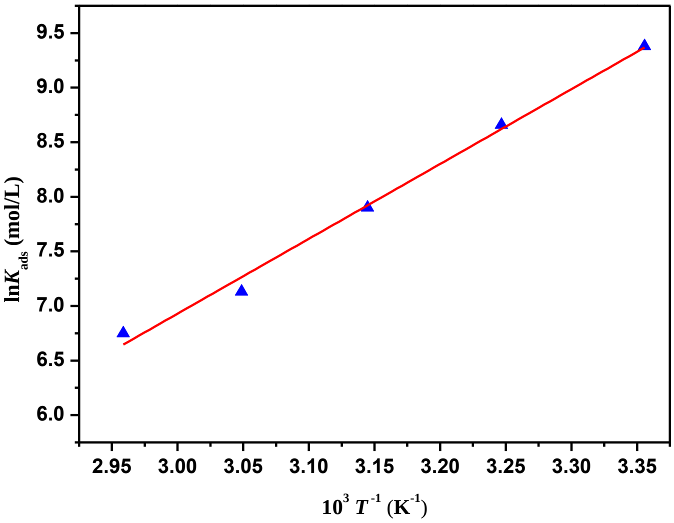

Figure 5. Plot of $\ln K_{\text{ads}}$ vs. $1/T$ for lepidine.

Table 4. Thermodynamic parameters of carbon steel in HCl solution

T (K)	K_{ads} (10^4 L/mol)	ΔG^0_{ads} (kJ/mol)	ΔH^0_{ads} (kJ/mol)	ΔS^0_{ads} (J/mol·K)
298	11.8	-33.2	-56.99	-79.96
308	5.78	-32.5		
318	2.69	-31.5		
328	1.25	-30.4		
338	0.699	-29.7		

The fitting curves of the weight loss test at different temperatures are showed in Fig. 4. The data calculated from the intercept are listed in Table 4. The enthalpy and entropy of the adsorption process were calculated according to eq. 10. Fig. 5 shows a plot of lnK_{ads} versus 1/T. The enthalpy and entropy of adsorption were obtained from the slope and intercept of the straight line, and the results are given in Table 4.

$$\ln K_{ads} = \ln\frac{1}{55.5} - \frac{\Delta H^0_{ads}}{RT} + \frac{\Delta S^0_{ads}}{R} \qquad \text{(eq. 10)}$$

The value of K_{ads} indicates the adsorption capacity of the inhibitor. As seen in Table 4, K_{ads} is higher at 298K, and this means that the adsorption of the inhibitor is both facile and strong. The negative value of ΔG^0_{ads} indicates that the adsorption of inhibitor on the steel surface is spontaneous. Generally, the value of ΔG^0_{ads} is less than -20 kJ/mol and close to -40 kJ/mol, and it can be assumed that a physisorption process (induced by electrostatic interactions between the inhibitor and charged metal surface) and a chemisorption process (charge sharing and transfer from the organic molecules to the metal surface to form a coordinate bond) are involved in the adsorption process[31-33]. Furthermore, because the value of ΔH0ads is negative, the adsorption process is exothermic, and increasing the temperature increases the rate of desorption. In addition, the negative value of ΔS^0_{ads} indicates that the inhibitor molecules are adsorbed on the surface of carbon steel in an ordered way[34].

3.5 Surface analysis

SEM images of the morphology of carbon steel are shown in Fig. 6. As seen in Fig. 6a, the surface of carbon steel after abrasion is smooth and the scratches are clear. After 3 h of immersion in acidic solution without inhibitor, the surface is severely corroded (Fig. 6b). With the addition of inhibitor, the carbon surface was protected (Fig. 6c). This preservation of the surface morphology explains the formation of a proper protective inhibitor film of lepidine on the carbon steel surface.

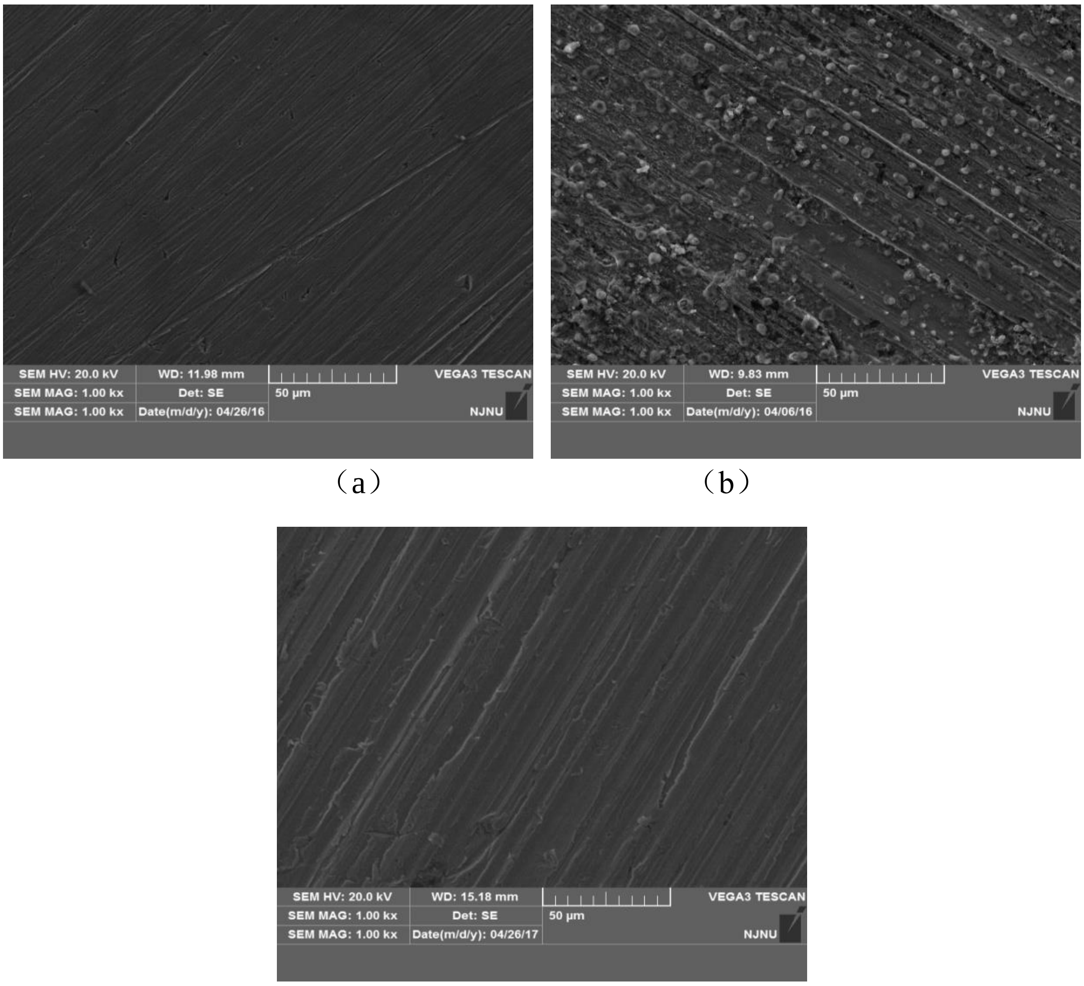

（a） （b）

（c）

Figure 6. SEM morphology of carbon steel after immersion in HCl solution with corrosion inhibitor: (a) after abrasion, (b) blank, and (c) with lepidine.

XPS was used to investigate the composition of the lepidine-adsorbed layer on the surface of carbon steel in 1 mol/L HCl medium. In this way, the high-resolution peaks for C 1s, O 1s, N 1s, and Fe 2p for the surface of carbon steel after 24 h of immersion were recorded and are given in Fig. 7a-e.

The high-resolution C 1s spectrum (Fig. 7b) shows two deconvoluted peaks as follows: the first peak is assigned to aliphatic carbons (-C-C-, -C=C-, and -C-H at 284.6 eV), and the second peak is assigned to the carbon atoms bonded to nitrogen in C-N and C=N bonds in the quinoline ring at 288.2 eV[35,36]. The N 1s XPS spectrum is fitted to two components (Fig. 7c), located at 399.2 eV and 401.2 eV. The component is mainly attributed to the C-N bonds in the quinoline ring and the quinoline ring coordinated with the steel surface (N-Fe) [37-40]. The O 1s spectrum for the carbon steel surface after it was immersed in test solution appears in three chemical states. The first peak, which is located at lower binding energy (529.9 eV), can be attributed to O^{2-}, and in principle, this can be related to the bond with Fe^{3+} in Fe_2O_3 and/or Fe_3O_4 oxides[41]. The second peak, which is located at approx. 531.5 eV, is ascribed to OH^- and can be attributed to oxygen in hydrous iron oxides, such as FeOOH and/or $Fe(OH)_3$[42]. The Fe 2p spectrum exhibits two peaks at 710.7 and 724.3 eV for Fe 2p3/2 and Fe 2p1/2, respectively, and these are attributed to ferric compounds such as Fe^{3+} oxides (e.g., Fe_2O_3 and Fe_3O_4) and oxyhydroxides (e.g., FeOOH)[43,44]. XPS results of the surface confirm that the anti-corrosion performance is mainly attributed to adsorption of the inhibitor.

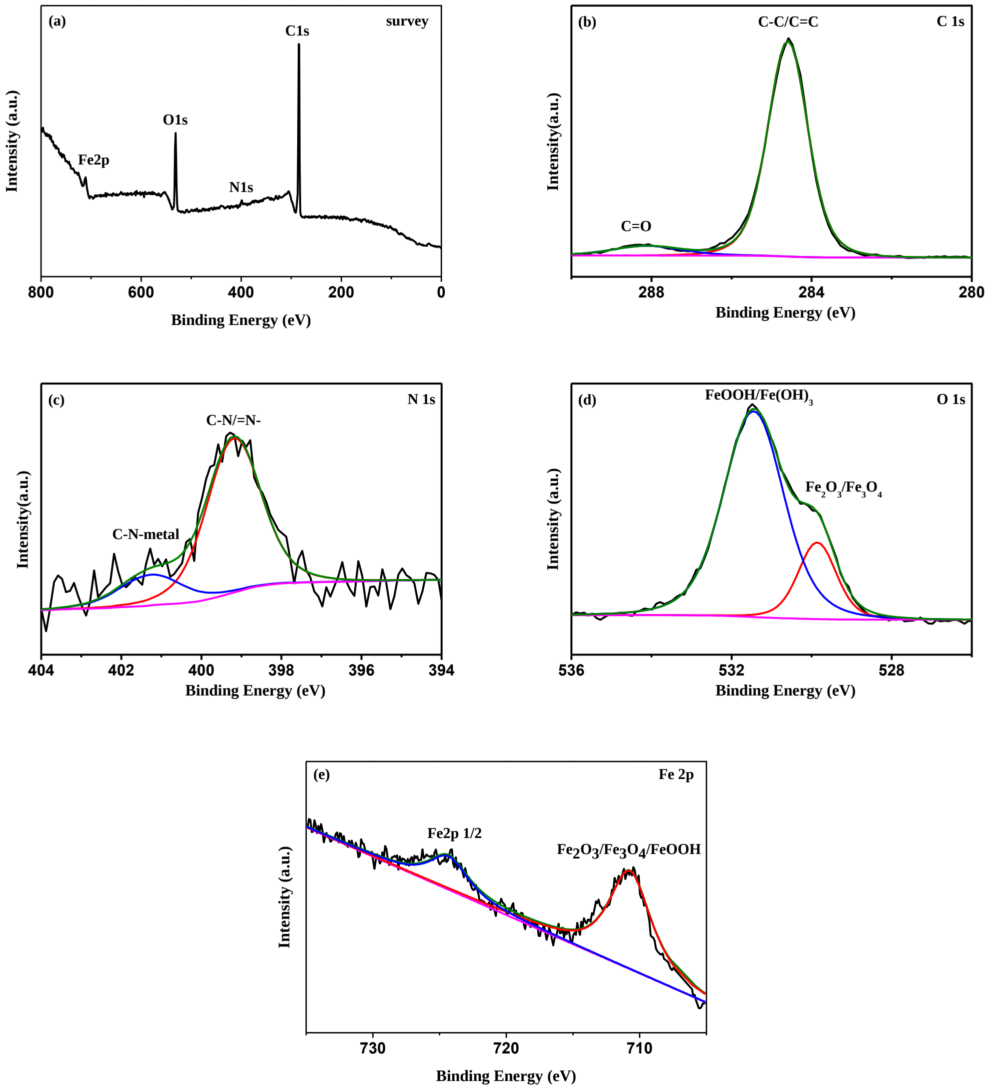

Figure 7. (a) XPS full spectrum. (b) C 1s, (c) N 1s, (d) O 1s, and (e) Fe 2p (e) high-resolution spectra of the surface of carbon steel.

4. CONCLUSIONS

(1) Lepidine is an effective inhibitor for carbon steel in 1 mol/L HCl solution at different temperatures. The inhibition efficiency increases with an increase in the concentration of inhibitor and reaches maximum values of 99.2% (EIS test) and 87.1% (potentiodynamic polarization curves) at the optimum concentration of 10 mmol/L.

(2) Polarization curves suggest that lepidine acts as a mixed-type inhibitor. Electrochemical impedance results show that corrosion inhibition of carbon steel in 1 mol/L HCl solution occurs via an adsorption process.

(3) Large negative values of $\Delta G^0_{\mathrm{ads}}$ indicate that adsorption of lepidine on the surface of carbon

steel is spontaneous, and the adsorption mechanism is physisorption and chemisorption. Adsorption of lepidine obeys the Langmuir adsorption isotherm.

ACKNOWLEDGMENTS

The author gratefully acknowledges the support of Key Founding of Sichuan Province Education Department (17ZA0220), Doctor Founding of Neijiang Normal University (No. 15B13), and the Opening Foundation of Key Laboratory of Fruit Waste Treatment and Resource Recycling of the Sichuan Province College (KF17004).

References

1. D. Daoud, T. Douadi, H. Hamani, S. Chafaa and M. Al-Noaimi, *Corros. Sci.*, 94 (2015) 21.
2. E. Gutierrez, J. A. Rodriguez, J. Cruz-Borbolla, J. G. Alvarado-Rodríguez and P. Thangarasu, *Corros. Sci.*, 108 (2016) 23.
3. M. Finsgar and D. K. Merl, *Corros. Sci.*, 83 (2014) 164.
4. A. Doner, R. Solmaz, M. Ozcan and G. Kardas, *Corros. Sci.*, 53 (2011) 2902.
5. A. Hejazi, Sh. Mohajernia, M. H. Moayed, A. Davoodi, M. Rahimizadeh, M. Momeni, A. Eslami, A. Shiri and A. Kosari, *J. Ind. Eng. Chem.*, 25 (2015) 112.
6. A. O. Yuce, B. D. Mert, G. Kardas and B. Yazici, *Corros. Sci.*, 83 (2014) 310.
7. H. M. Abd El-Lateef, M. A. Abo-Riya and A. H. Tantawy, *Corros. Sci.*, 108 (2016) 94.
8. G. Moretti, F. Guidi and F. Fabris, *Corros. Sci.*, 76 (2013) 206.
9. W. S. Guo, L. H. Cheng and Y. F. *Cong, Surf. Tech.*, 47 (2018) 188.
10. L. Jiang, Y. J. Qiang and Z. L. Lei, *J. Mol. Liq.*, 255 (2018) 53.
11. I. B. Obot, N. K. Ankah and A. A. Sorour, *Sustain. Mater. Tech.*, 14 (2017) 1.
12. T. J. Harvey, F. C. Walsh and A. H. Nahle, *J. Mol. Liq.*, 266, (2018) 160.
13. P. Singh, V. Srivastava and M. A. Quraishi, *J. Mol. Liq.*, 216 (2016) 164.
14. H. Lgaz, R. Salghi and K. S. Bhat, *J. Mol. Liq.*, 244 (2017) 154.
15. I. B. Obot and N. O. Obi-Egbedi, *Curr. Appl. Phys.*, 11 (2011) 382.
16. A. Singh, Y. H. Lin, I. B. Obot E. E. Ebenso, K. R. Ansari and M. A. Quraishi, *Appl. Surf. Sci.*, 356 (2015) 341.
17. L. Fragoza-Mar, O. Olivares-Xometl, M. A. Dominguez-Aguilar, E. A. Flores, P. Arellanes-Lozada and F. Jimenez-Cruz, *Corros. Sci.*, 61 (2012) 171.
18. M. Hosseini, S. F. L. Mertens, M. Ghorbani and M. R. Arshadi, *Mater. Chem. Phys.*, 78 (2003) 800.
19. N. Labjar, M. Lebrini, F. Bentiss, N. E. Chihib, S. El Hajjaji and C.Jama, *Mater. Chem. Phys.*, 119 (2010) 330.
20. F. Bentiss, M. Lebrini and M. Lagrenee, *Corros. Sci.*, 47 (2005) 2915.
21. Z. Y. Cao, Y. M. Tang, H. Cang, J. Q. Xu, G. Lu and W. H. Jing, *Corros. Sci.*, 83 (2014) 292.
22. D. K. Yadav, M. A. Quraishi and B. Maiti, *Corros. Sci.*, 55 (2012) 254.
23. V. V. Torres, V. A. Rayol, M. Magalhaes, G. M. Viana, L. C. S. Aguiar, S. P. Machado, H. Orofino and E. D'Elia, *Corros. Sci.*, 79 (2014) 108.
24. F. B. Growcock and R. J. Jasinski, *J. Electrochem. Soc.*, 136 (1989) 2310.
25. M. Outirite, M. Lagrenee, M. Lebrini, M. Traisnel, C. Jama, H. Vezin and F. Bentiss, *Electrochim. Acta,* 55 (2010) 1670.
26. M. A. Hegazy, A. M. Badawi, S. S. Abd El Rehim and W. M. Kamel, *Corros. Sci.*, 69 (2013) 110.
27. S. S. Shivakumar and K. N. Mohanam, *Corros. Sci.*, 13 (2013) 1.
28. R. Solmaz, E. Altunbas and G. Kardas, *Mater. Chem. Phys.*, 125 (2011) 796.
29. A. O. Yuce and G. Kardas, *Corros. Sci.*, 58 (2012) 86.
30. A. Asan, M. Kabasakaloglu, M. Isiklan and Z. Kilic, *Corros. Sci.*, 47 (2005) 1534.

31. H. M. Abd El-Lateef, V. M. Abbasov, L. I. Aliyeva, E. E. Qasimov and I. T. Ismayilow, *Mater. Chem. Phys.*, 142 (2013) 502.
32. M. K. Pavithra, T. V. Venkatesha, M. K. Punith Kumar and H. C. Tondan, *Corros. Sci.*, 60 (2012) 104.
33. I. Jevremovic, M. Singer, S. Nesic and V. Miskovic-Stankovic, *Corros. Sci.*, 77 (2013) 265.
34. M. Abdallah, *Corros. Sci.,* 44 (2002) 717.
35. J. F. Watts and J. Wolstenholme, An introduction to surface analysis by XPS and AES, John Wiley and Sons Inc., (2003) London, UK.
36. C. Wagner, W. M. Riggs, L. E. Davis, J. F. Moulder and G. E. Muilenberg, Handbook of X-Ray photoelectron spectroscopy, Perking-Elmer Corporation, Physical Electronics Division, (1979) Minnesota, US.
37. E. T. Kang, K. G. Neoh and K. L. Tan, *Surf. Interface Anal.*, 19 (1992) 33.
38. M. Lebrini, M. Lagrenee, M. Traisnel, L. Gengembre, H. Vezin and F. Bentiss, *Appl. Surf. Sci.*, 253 (2007) 9267.
39. A. G. Schick and Z. Sun, Langmuir, 10 (1994) 3105.
40. R. Devaux, D. Vouagner, A. M. De Becdelievre, C. Duret-Thual, *Corros. Sci.*, 36 (1994) 171.
41. F. Bentiss, M. Traisnel, L. Gengembre and M. Lagrenee, *Appl. Surf. Sci.*, 161 (2000) 194.
42. W. Temesghen and P. M. A. Sherwood, *Anal. Bioanal. Chem.*, 373 (2002) 601.
43. M. A. Pech-Canul and P. Bartolo-Perez, *Surf. Coat. Tech.*, 184 (2004) 133.
44. F. Z. Bouanis, F. Bentiss, M. Traisnel and C. Jama, *Electrochim. Acta*, 54 (2009) 2371.